



Tool-integrated thin-film sensor systems for measurement of cutting forces and temperatures during machining

Marcel Plogmeyer^{1,2} · Germán González³ · Christina Pongratz^{1,2} · Anna Schott² · Volker Schulze³ · Günter Bräuer¹

Received: 29 September 2023 / Accepted: 5 December 2023 / Published online: 13 January 2024
© The Author(s) 2024

Abstract

Effective in-process control mechanisms are vital for the future development of production processes and ask for reliable monitoring of process variables. For this, new tool-integrated sensor systems for measuring cutting forces and temperature for machining of hardened steel are proposed. Thin-film technology is used to apply a thermoresistive temperature sensor in the chip-workpiece contact area for the first time on industrial cutting inserts with chip breaker geometry. Complementary piezoresistive thin-film sensors based on diamond-like carbon (DLC) and manganin layers were developed and deposited on a washer. It was placed beneath the indexable insert to measure the cutting forces. Turning experiments were conducted to study sensor life and accuracy. All sensors showed an adequate lifetime for laboratory purposes. Temperature compensation methods were investigated for force measurement and results compared to forces recorded by a dynamometric platform. While temperature compensation for the DLC-based sensor needs further optimization, results of the manganin-based sensor compared well with the expected cutting forces. The manganin thin-film sensor exhibited rapid responsiveness and great reproducibility, underscoring its prospective utility for real-time monitoring of cutting forces in machining operations.

Keywords Thin-film sensor · Machining · Force measurement · Temperature measurement

1 Introduction

Measurement of cutting forces and process temperatures during machining provides critical insights into the physical principles governing the process. In laboratory settings, piezoelectric dynamometric platforms are typically employed for acquiring cutting force data. However, their high costs, substantial size, and sensitivity often restrict their practical application in real-world use. As a result, numerous studies have been conducted to explore alternative methods for measuring cutting forces. This work will concentrate on technologies based on thin-film sensors, which hold significant promise due to their compact size and potential for

scalable production. Klocke et al. [1] explored the integration of a piezoelectric force sensor within a tool holder specifically designed for turning operations. Positioned directly beneath the cutting insert, the sensor underwent a series of machining tests to evaluate its efficiency. Subsequently, the data acquired from these tests were benchmarked against readings from a plate dynamometer to ascertain comparative performance. Drossel et al. [2] used a piezoelectric thick film sensor for measuring cutting forces during milling in the direct vicinity of an indexable insert. A carbide plate was coated with a piezoceramic thick film sensor layer of lead zirconate titanate (PZT) and mounted behind the insert. Tests showed good correlation between the developed sensor system and a conventional dynamometer. A PZT sensor was also taken by Panesso et al. [3] to measure the quasistatic cutting forces in turning processes. It was integrated between the tool-holder and the tool-holder receptacle. Cheng et al. [4] mounted thin-film strain sensors based on NiCr alloy onto three different kind of tool bars. The thin-film sensors were coated onto elastic substrates of various designs. Experimental tests were conducted with static loads.

Beyond applications in turning processes, Biehl et al. used an amorphous DLC layer for static and dynamic force

✉ Marcel Plogmeyer
m.plogmeyer@tu-braunschweig.de

¹ Institute for Surface Technology (IOT), TU Braunschweig, Riedenkamp 2, 38108 Braunschweig, Germany

² Fraunhofer Institute for Surface Engineering and Thin Films IST, Riedenkamp 2, 38108 Braunschweig, Germany

³ wbk Institute of Production Science, Karlsruhe Institute of Technology (KIT), Kaiserstr. 12, 76131 Karlsruhe, Germany

measurements in screw connections [5] and on the surface of tools in forming processes [6]. In addition to excellent tribological properties (hardness of 35 GPa, abrasive wear below $1 \cdot 10^{-15} \text{ m}^3/\text{Nm}$), this DLC layer exhibits a clear piezoresistive effect. It shows a linear resistance dependence on the load, which opens up a wide range of sensory application possibilities. The layer is deposited directly onto steel base bodies in plasma-enhanced chemical vapor deposition (PECVD) processes. When combined with structured metal electrodes and an insulating and wear-protective hydrocarbon layer modified with silicon and oxygen, it forms a wear-resistant piezoresistive thin-film sensor system.

The DLC layer mentioned above exhibits also thermoresistive properties, thus requiring a temperature compensation for correct measurements. This can be circumvented with an alternative sensor material like manganin, which is an alloy of 84–86% copper, 12% manganese and 2–4% nickel [7]. Manganin has a very small temperature coefficient of resistance in the order of 10^{-5} 1/K and a linear pressure coefficient of up to $2.5 \cdot 10^{-5} \text{ 1/MPa}$ [8], which makes it an ideal material for pressure sensors that are subject to dynamic temperature changes. It has been used to investigate lubricated contacts in bearings [9] or on gear wheels [10], where pressures of several 100 MPa occur but also temporary temperature rises of up to 100 K. The thin-film systems consisted of a thin manganin layer which was placed in between two insulating aluminium oxide layers.

The utilization of thin-film sensors to measure process temperatures in proximity to the cutting zone during turning processes has been effectively demonstrated, as evidenced by González et al. [11]. They also provided a comprehensive overview of various thin-film methods for temperature measurement. These methods primarily rely on the thermoelectric effect [12] and the thermoresistive effect [13]. However, none of the previous studies have been conducted on cutting inserts with chip breaker geometries, which pose unique challenges for the coating and structuring processes of the sensors. Beside wear and delamination of the thin-film system, strain and plastic deformation can impact the lifetime and usability of thin-film sensors. Ottermann et al. [14] suggested a method to correct changes of the temperature coefficient due to plastic deformation and thereby prolong the usability of thin-film sensors.

In this paper, we introduce a novel methodology for measuring machining forces using sensors derived from thin-film technology. This involves the implementation of two distinct piezoresistive thin-film systems positioned on a washer beneath the cutting insert. Given the significant impact of temperature fluctuations on these sensors, we also introduce a model for temperature compensation. The effectiveness of these sensors is evaluated by comparing the forces recorded during the turning tests with those measured using a dynamometric platform. Furthermore, we propose a

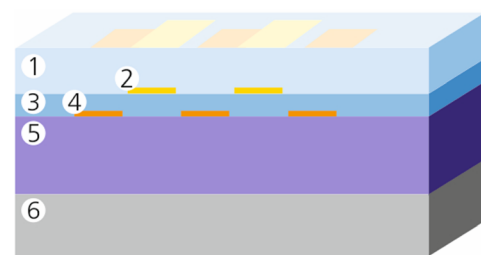
new approach to fabricate thermoresistive thin-film sensors on cutting inserts with chip breaker geometries, building upon the techniques outlined in previous research [11]. This paper details the manufacturing process, characterization, and the practical testing of these sensors in turning experiments on AISI 4140 Q & T workpieces.

2 Piezoresistive force sensor

This section outlines the deposition process, design and calibration process of the two types of force sensors developed in the study.

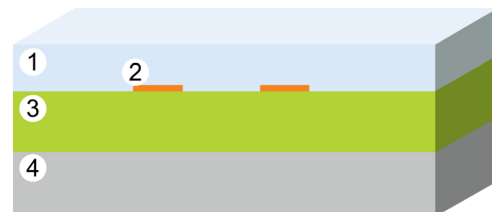
2.1 Deposition of DLC sensor

A schematic view of the piezoresistive thin-film system is given in Fig. 1a. It is based on a $6 \mu\text{m}$ DLC layer (5) with piezoresistive properties which was deposited on the metal base body of the sensory washers (6) in a plasma enhanced chemical vapor deposition (PECVD) process. The material of the washer is DIN 1.3343 high-speed-steel with hardness



- 1 Insulating and wear-protection layer ($3 \mu\text{m}$)
- 2 Conductor paths and contact pads ($0.2 \mu\text{m}$)
- 3 Insulating and wear-protection layer ($1 \mu\text{m}$)
- 4 Electrode structure Cr ($0.2 \mu\text{m}$)
- 5 Piezoresistive DLC layer ($6 \mu\text{m}$)
- 6 Metal base body

(a) Piezoresistive thin-film system of a DLC sensor



- 1 Insulating and wear-protection layer ($3 \mu\text{m}$)
- 2 Meander structure Manganin ($0.2 \mu\text{m}$)
- 3 Insulating Al_2O_3 layer ($4 \mu\text{m}$)
- 4 Metal base body

(b) Thin-film system of a manganin sensor

Fig. 1 Piezoresistive thin-film systems for measurement of forces

of 64–66 HRC. Force and temperature compensating electrodes (4) were implemented using a chromium layer which was deposited with a thickness of 200 nm by sputtering. This chromium layer was structured using photolithographic processes and wet chemical etching. Next, an intermediate insulating amorphous hydrocarbon layer modified with oxygen and silicon (3) was deposited using PECVD with a thickness of 1 μm , followed by the deposition of another chromium layer (2). The second chromium layer was structured in the shape of conductor paths, connecting the force and temperature compensating (TC) electrodes with the associated contact pads. The whole sensor system was protected by a final insulating and wear-protecting layer (1). The contact pads were covered during the deposition of the top layer, allowing a copper layer to be deposited so that wires could be soldered to the sensors.

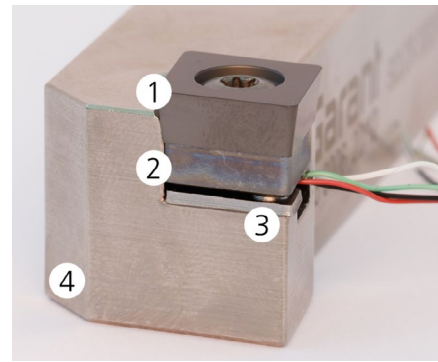
2.2 Deposition of manganin sensor

The thin-film system of the manganin sensor is shown in Fig. 1b. Because of the differing measurement principle, its structure is also different and resembles that of the temperature sensors presented in the next chapter. At first, an insulating layer of aluminium oxide (3) with a thickness of 4 μm was deposited on the metal base body of the sensory washer (4) by physical vapour deposition (PVD). Next, the manganin sensor (2) was structured in a lift-off process. A photoresist was applied on top of the aluminium oxide layer and structured using photolithography. After sputtering of a 200 nm thick layer from a manganin target (86% copper, 12% manganese and 2% nickel), the resist was stripped and the sensor structure remained. The same insulating and wear-protecting layer as for the DLC sensor was applied in the end.

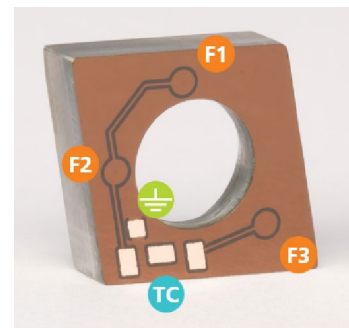
2.3 DLC sensor design

To measure the cutting force, a sensor system consisting of a sensory washer (2) with the thin-film system on its bottom and a profiled washer (3) were placed underneath the indexable insert (1) (see Fig. 2a). The profiled washer directed force to the sensor structures, increasing local pressure for better sensitivity. Three circular points of contact were chosen to avoid tilting. The tool holder (4) was modified so that the wires could be soldered to the bottom of the sensory washer.

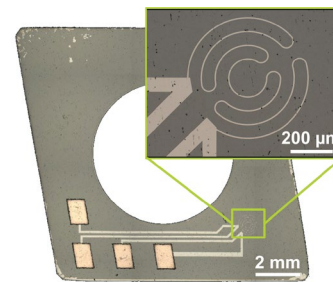
On the sensory washer for the DLC sensor, three force (F) electrodes and one temperature compensating (TC) structure were included. They were used to measure the resistance through the piezoresistive DLC layer to the base body. Each force electrode was placed at a point of contact with the profile washer. One electrode (F3) was positioned underneath the washer at the side of the tool engagement point (see



(a) Sensor system consisting of the indexable insert (1), sensory washer with coated thin-film system on its bottom (2) and profiled washer (3), placed within a modified tool holder (4)



(b) DLC sensor design with three force electrodes (orange) of which two are connected in parallel (F1 and F2), a temperature compensating structure (blue) and a physical ground connection (green)



(c) Manganin sensor design with a meandering sensor structure

Fig. 2 Sensor implementation and designs for cutting force measurement with a sensory washer

Fig. 2b). The other two electrodes (F1+F2) were structured on the opposite side and electrically connected in parallel due to space limitations.

An electrode for temperature compensation was included alongside the force sensors to ensure accurate measurements. The piezoresistive layer is sensitive to both force and temperature, making it necessary to differentiate between

the two. To prevent measuring force as temperature-related resistance changes, the temperature compensation electrode is located outside the force flow of the profiled washer. This ensures that it is not subjected to any force and any resistance changes detected can be attributed solely to temperature.

To determine the actual cutting force, there are two methods to separate the temperature influence from the measured resistance. On the one hand, temperature compensation can be achieved through a voltage divider. In this case, the temperature compensating resistance and the force resistance were connected in series. Thus, the changes in resistance due to changes in temperature were applied to both electrodes and were therefore cancelled out in the output voltage. On the other hand, both resistances could be acquired separately, followed by a mathematical correction of the resistance of the force sensor using the temperature compensating structure. In both cases, the temperature at the electrodes is required to be the same.

2.4 Manganin sensor design

To measure the resistance of the manganin sensor, four-wire sensing was used. Thereby, only the resistance of the meandering sensor structure is measured. The meandering structure consists of a 10 μm wide conducting path and is located underneath the washer at the side of the tool engagement point (see Fig. 2c). This is the same position as electrode F3 of the DLC sensor.

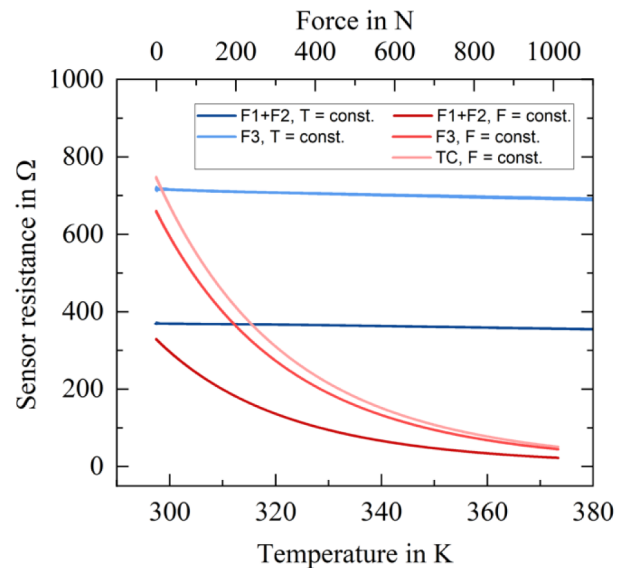
2.5 Calibration procedure

2.5.1 Force dependency

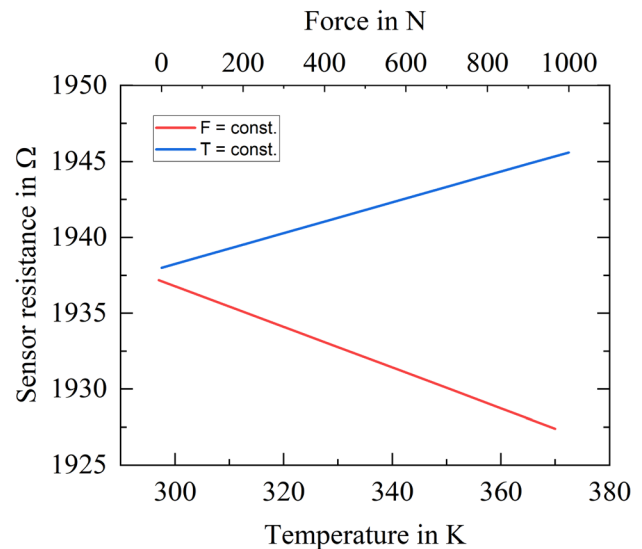
For the characterization of the force dependency, the profiled washer and a sensory washer were mounted onto the tool holder. A force of up to 1 kN was applied on the surface with a servo press. The change of the resistances was recorded using a voltage divider for the DLC sensor, set up by the TC structure and the force electrodes. The resistance of the manganin sensor was measured by four-wire sensing. The linear behaviour of both sensor types (see Fig. 3) can be described by the following equation:

$$R(F) = R(F = 0) \cdot [1 + K^* \cdot F] \quad (1)$$

K^* is the normalized force coefficient and is independent of the output resistance. The measured values are $K_{F1+F2}^* = -3.65 \cdot 10^{-5} 1/\text{N}$ and $K_{F3}^* = -1.09 \cdot 10^{-5} 1/\text{N}$ for the DLC sensors and $K_M^* = 3.53 \cdot 10^{-6} 1/\text{N}$ for the manganin sensor. The differences in sensitivity between the F1+F2 electrode and the F3 electrode could be attributed to various reasons, such as slight misplacement of the profiled washer and electrodes, a slight tilting of the profiled washer



(a) DLC sensor



(b) Manganin sensor

Fig. 3 Calibration curves of the piezoresistive thin-film systems

or differences in layer properties over the sensory washer. In general, the sensitivity of the DLC force sensors is significantly higher than that of the manganin sensor. However, one disadvantage of the DLC sensor is the strong temperature dependence of the resistances in contrast to the manganin sensor as described in the following section.

2.5.2 Temperature dependency

For both force sensors, the thermoresistive behaviour was recorded by placing the sensory washers inside a laboratory

oven, which was heated up to 100 °C. The cooling curve was recorded and the resistances were measured. The reference temperature was measured using a Pt100 sensor.

The DLC layer has semiconducting properties and thus behaves like a negative temperature coefficient (NTC) thermistor. The behaviour can be described by the Steinhart-Hart equation [15]:

$$\frac{1}{\{T\}} = A + B \cdot \ln\{R\} + C \cdot (\ln\{R\})^3 \quad (2)$$

In this numerical-value equation the value of temperature T is given in Kelvin and the value of the resistance R in Ω . An example of the thermoresistive characteristic is depicted in Fig. 3a. Force and TC structures have different output resistances but otherwise show the same behaviour.

Manganin, as mentioned in the introduction, has a very small temperature coefficient compared to other metals. Since the expected force values in the experiments are relatively small, it has to be accounted for. The behaviour can be approximated by a linear equation:

$$R(T) = R_0 \cdot [1 + \alpha \cdot (T - T_0)] \quad (3)$$

The temperature coefficient α at temperature $T_0 = 273.15$ K was $\alpha = -6.8 \cdot 10^{-5}$ 1/K for the manganin sensor.

3 Thermoresistive thin-film sensors

3.1 Deposition

The thermoresistive temperature sensors were placed on the rake face of industrial cutting inserts with chip breaker geometry (CCMT120404-RP4). The used cutting inserts were provided with the Tiger.tec® Silver coating by Walter Tools. It includes an aluminium oxide layer for wear protection purposes. Preliminary tests showed that the adhesion of the sensor system was improved compared to inserts without a pre-coating. In order to ensure the electrical insulation of the sensors from the metal base body, an additional layer of aluminium oxide with a thickness of 1 μm was deposited on the rake face in a PVD process. The subsequent 200 nm thick chromium layer was structured using photolithography and wet chemical etching. The sensors are protected from external influences by another layer of aluminium oxide with a thickness of 2 μm . The contact pads were coated with copper. This allowed cables to be soldered to the contact pads.

3.2 Design and structuring

Two temperature sensors were structured on the rake face with the aim to measure the temperature and its gradient. Both were designed as a meandering structure and cover an area

of 140 $\mu\text{m} \times 140 \mu\text{m}$ (see Fig. 4). The sensors were placed 2000 μm (TM1) and 2250 μm (TM2) from the cutting edge. This is in front of the chip breaker, since its edge was identified as a high risk for interrupted conducting paths regarding the very thin sensor structures. The placement would also lead to a longer sensor lifetime, as less wear was expected than in the tool-chip contact zone. In future work, it will be the aim to place the sensors on the chip breaker itself. Due to space limitations on the planar part of the rake face, the contact pads for the cables soldered to the sensor structures were placed within the chip breaker geometry.

The structuring of the temperature sensors was implemented similar to previous works by using a photoresist that was applied by electrophoretic deposition (EPD) [11]. The advantage of the EPD process is an almost uniform resist thickness, which cannot be achieved by spin-coating or air-brush deposition due to the chip breaker geometry of the cutting inserts examined in this study. The photolithographic structuring of the resist was done by direct laser exposure with a Nd:YAG laser (LS9000 from the manufacturer LaserSystems) at a wavelength of 355 nm. The benefit of this technique is that it can be used to structure more complex shaped surfaces, such as the cutting inserts with chip breaker geometry, which cannot be done with a glass mask. Still, line widths of down to 10 μm were feasible, enabling the production of sensors with excellent spatial resolution.

3.3 Calibration procedure

Similar to the force sensors, the temperature sensors were characterized in a laboratory oven. Figure 5 shows the thermoresistive characteristic. The sensors behave like a positive temperature coefficient (PTC) thermistor and their behaviour can be described by the following function:

$$R(T) = R_0 \cdot [1 + \alpha \cdot (T - T_0) + \beta \cdot (T - T_0)^2] \quad (4)$$

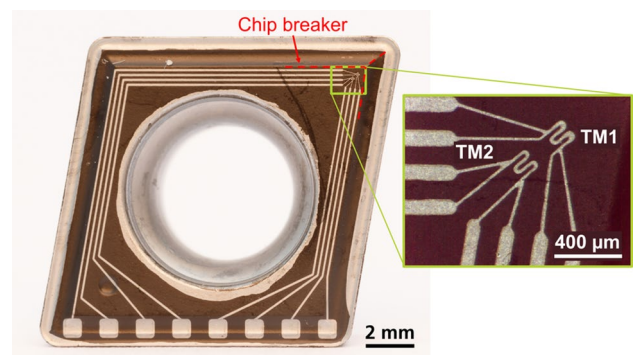


Fig. 4 Thin-film sensor system for measurement of temperatures

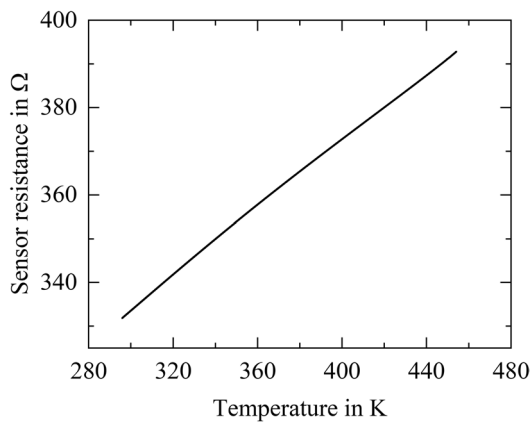


Fig. 5 Temperature calibration curve of a thermoresistive temperature sensor

The temperature coefficients α and β as well as the output resistance R_0 at temperature $T_0 = 273.15$ K were determined for each sensor. On average, the values of the temperature coefficients were $\alpha = 1.3 \cdot 10^{-3}$ 1/K and $\beta = -0.7 \cdot 10^{-6}$ 1/K².

4 Experimental setup and tests

Dry cutting experiments were conducted on a CNC turning center Index G200 using cylindrical specimens made of AISI 4140 Q & T. Process parameters are given in Table 1. Figure 6 shows the experimental setup and the sensor technology used. A dynamometric platform Kistler 9257B was used with a sampling frequency of 10 kHz. Thin-film force and temperature sensors presented in Sections 2 and 3 were integrated into the tool system. Carbide inserts type CCMT120404-RP4 Tiger.tec[®] with substrate Grade P30 WC and with a cutting edge radius r_β of 45 ± 5 μm from the company Walter Tools were used. A 1 mm thick thermally insulating ceramic plate was added in between the indexable insert and the sensory washer in order to reduce the temperature influence on the thin-film force sensor. The resistances of the force and TC structures of the DLC sensor were measured by setting up a voltage divider with a constant resistance for each structure. A CompactDAQ from National Instruments was used in combination with a NI-9205 module to measure the voltage drops across each structure at a sampling rate of 10 kHz, from which the resistances were calculated. This allowed a mathematical correction of the

Table 1 Longitudinal turning: process parameters

	Rake angle γ	Clearance angle α	Main cutting angle κ	Cutting fluid
	0°	7°	95°	none
		Cutting speed v_c in m/min	Feed rate f in mm/rev	Depth of cut a_p in mm
Force sensor tests		100	0.20, 0.30	0.3, 0.6, 0.9
Temperature sensor tests		100, 150, 200	0.10, 0.20	0.6

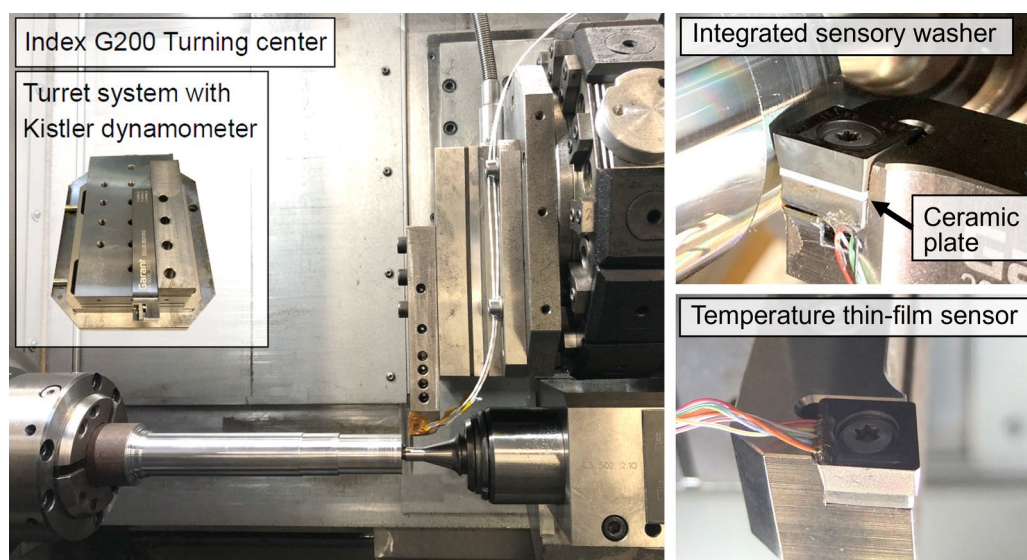


Fig. 6 Experimental setup for longitudinal turning

temperature influences following the measurement. A four-wire configuration was used for measuring the resistance of the manganin and thermoresistive sensor. A Keithley 2601 was used as a current source applying a constant current of 1 mA to the sensor. The resulting voltage drop across the sensor was recorded using a NI-9223 module at a sampling rate of 10 kHz.

5 Results and discussion

5.1 Force measurement

In order to evaluate the two sensor concepts and designs with regard to sensitivity as well as efficiency of the temperature compensation, turning experiments with varying parameters were conducted with the sensory washers.

5.1.1 DLC sensor

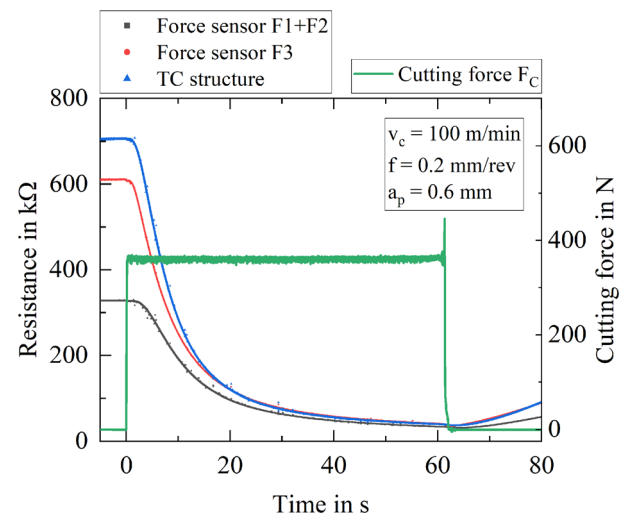
In Fig. 7a the raw signal output of the thin-film sensors as well as the cutting force F_C of the dynamometer is shown for an exemplary measurement. It can be seen that both the force sensors and TC resistances dropped significantly during the cut. This was mainly due to the heat input because the DLC layer is much more sensitive to temperature changes than to force changes, as could be deduced from the preliminary calibrations.

Therefore, the temperature-compensated force signals were calculated with the following equation:

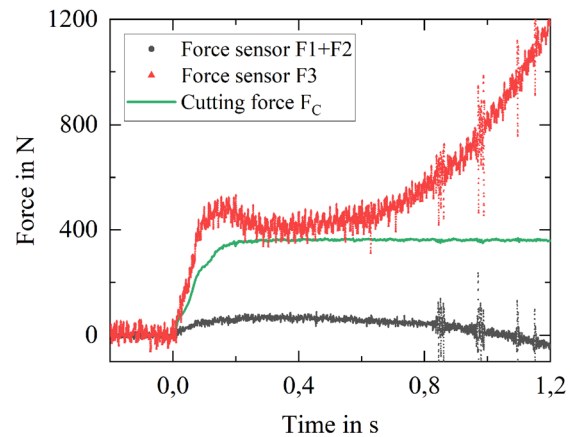
$$R_{F,comp} = \frac{R_F \cdot R_{TC}(t = 0)}{R_{TC}} \quad (5)$$

Those values were used to calculate the sensor forces using equation 1 and a 500 Hz low-pass filter was applied. They are depicted in Fig. 7b for the first 1.2 s. For F3 it can be seen, that the sensor force starts to increase at the same time as the cutting force measured with the dynamometer. After about 0.2 s, it reaches a temporary maximum value of about 500 N before decreasing to a value of little more than 400 N. This compares well to the steady state cutting force of 360 N. In contrast, the cutting force deduced from F1+F2 is much lower at below 100 N. It is assumed, that this observation is due to the cutting force acting on the cutting edge. The tool and the washer might tilt slightly and thus the force acts mainly on the profile at the position of F3. This might be corrected with a calibration done by turning experiments.

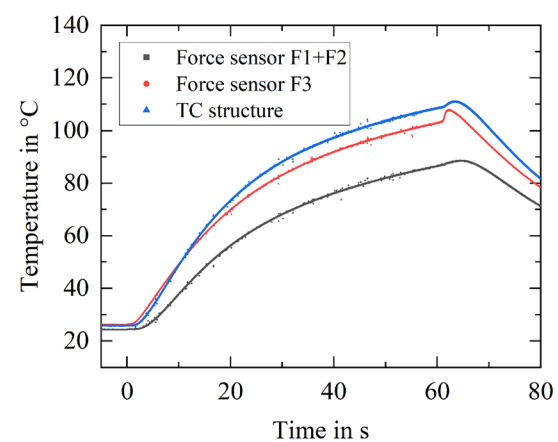
After a short processing time of less than 1 s, the force signal behaved unexpectedly, rising to much higher values (F3) and to negative values (F1+F2), respectively. This cannot be explained by the force impact, since the force measured with the dynamometer stayed constant throughout the



(a) Raw sensor signal



(b) Sensor forces calculated from temperature-compensated sensor signals



(c) Temperatures of the force sensor and TC structure

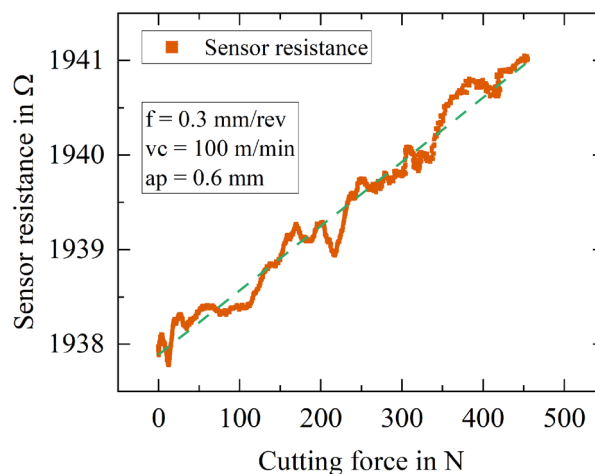
Fig. 7 Force and temperature measurements with the DLC thin-film sensor and dynamometer

cutting process. An estimation of the temperatures of both the force and the TC structures shows that there was a discrepancy between the prevailing temperatures over time (see Fig. 7c), making a temperature compensation during the entire cutting process practically unfeasible with the used sensor design. The difference is assumed to originate in the fact that, on the one hand, the force and TC structures were located apart from each other. The heat reached F1 and F2 later than F3 and the TC structure. On the other hand, the force structures were in contact with the profiled washer as opposed to the TC structure, resulting in heat dissipation and a lower temperature compared to the TC structure.

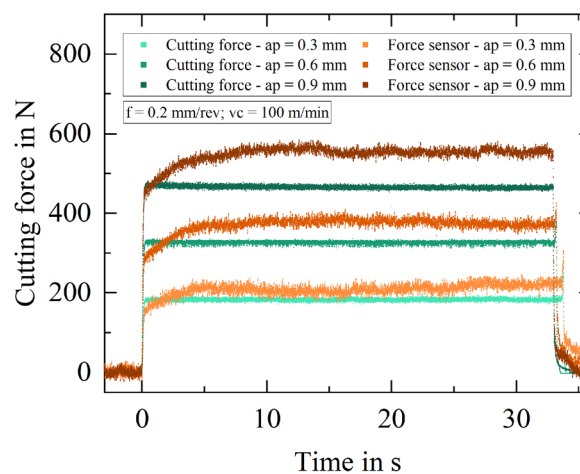
5.1.2 Manganin sensor

As was observed in the previous section, the location of the sensor seems to have an impact on the force transmitted by the profiled washer. Therefore, an additional calibration was conducted with the manganin sensor in the turning center for different feed rates and cutting depths (see Table 1). To mitigate potential thermal effects on the measurements, only the initial slope of the cutting force was taken into account, occurring within the first 0.1–0.2 s of the cut. This was achievable because the manganin sensor exhibited no latency compared to the dynamometer. Figure 8a shows an exemplary calibration curve. Despite significant noise due to the short measuring time, a linear behaviour could be observed, as was also the case in the laboratory calibration. On average, a normalized force coefficient of $K^* = 3.64 \cdot 10^{-6} \text{ 1/N}$ was determined, which is in good accordance with the value obtained in the laboratory calibration.

The evaluation of the sensor performance was subsequently done by conducting cutting experiments with three different depths of cut. The temperatures measured with the DLC sensor indicated a significant heat impact on the sensory washer. Although manganin has a very small temperature coefficient, a temperature difference of e.g. 50 K would lead to an error in calculated force of almost 1000 N. Initially, no temperature compensation was provided on the washer with the manganin sensor. Therefore, the exact same experiments were repeated with the DLC sensor to obtain from structure F3 the temperature profile at the position of the manganin sensor. The force impact on the overall resistance change is negligible compared to the heat impact (compare Fig. 3a). It amounts to only 0.15 K for a force of 360 N. The temperature profile was utilized to subtract the resistance change attributed to temperature fluctuations from the manganin signal. From the resulting temperature-compensated resistance, the sensor force was calculated using equation 1. In Fig. 8b, the sensor forces are compared to the cutting forces measured by the dynamometer. A lowpass filter was applied to reduce excessive noise.



(a) Calibration curve



(b) Sensor forces calculated from temperature-compensated sensor signals

Fig. 8 Calibration and force measurements with the manganin thin-film sensor and dynamometer

The manganin sensor shows very good initial response, but it takes 5–10 s until a steady state is reached. This delay might be attributed to minor temperature disparities observed in both the DLC and manganin sensor experiments. Consequently, the temperature compensation leads to underestimated force values until a leveling of temperatures is attained. Alternatively, it is plausible that thermal expansion of the materials involved could occur, thereby resulting in an augmentation of the pretensioning force. Moreover, the initial pretensioning force itself might alter the magnitude of the thermal expansion. Further investigations are warranted to explore this matter comprehensively. The fact, that a steady state was measured with the manganin sensor, indicates a successful temperature compensation for longer process times. Steady state forces

were systematically 10–20% higher than those measured by the dynamometer. This means, that the manganin sensor is able to detect the cutting forces qualitatively but only wrong by a constant factor. A correction of the force coefficient would lead to the quantitative right results. In future experiments, a calibration that uses the temperature compensated steady state signal, rather than the short time signal of the force rise, should lead to a more accurate force coefficient.

All experiments were repeated at least once and led to the same profiles, showing good reproducibility of the thin-film sensor.

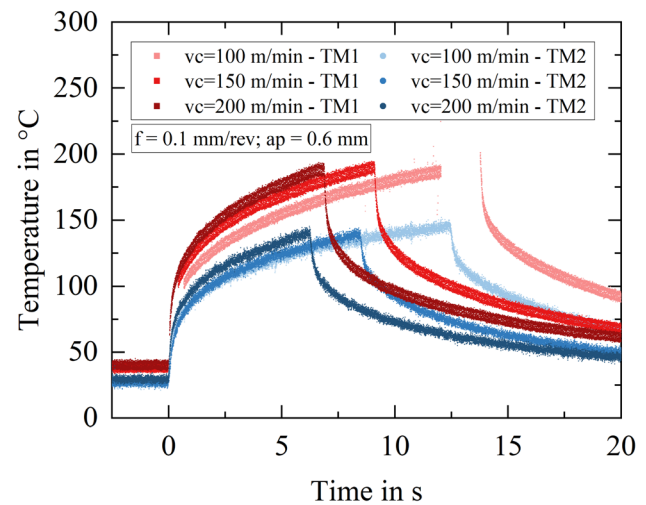
5.2 Temperature measurement

The functionality of the thermoresistive thin-film sensors was studied in turning processes under the different parameter combinations listed in Table 1.

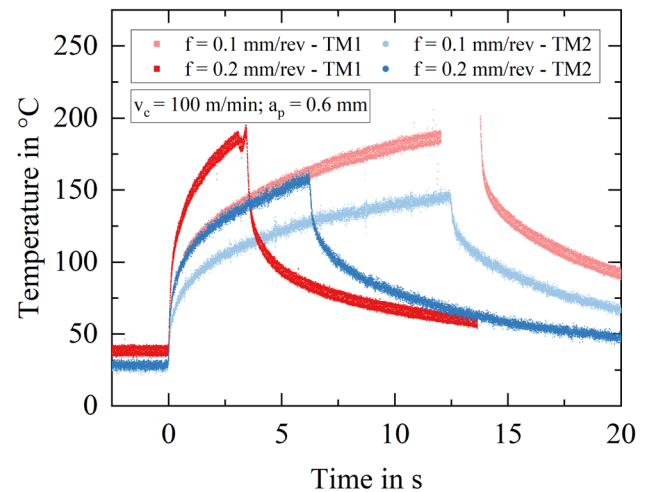
Unfortunately, inserts with two intact meander structures were not available due to short circuits or interruptions of the conducting paths that occurred during the fabrication process. Therefore, two separate inserts were utilised, one with sensor TM1 and the other with sensor TM2.

For both, experiments with the same cutting parameters were conducted once and compared. Since the number of cutting tests done with each insert was five, abrasive tool wear could be neglected.

The measured temperatures, after filtering out excessive noise due to a low output resistance of the sensor, are displayed in Fig. 9. Missing data points can be explained by temporarily shortages with the chip. Due to a slightly smaller workpiece diameter in experiments with the insert with TM2, cutting times were shorter for these. The temperatures of TM1 also have a small offset of 5–10 K in comparison to TM2 that might be explained by different ambient temperatures at the time of the experiments. This led to an overestimation equivalent to the offset of the TM1 signal. Nonetheless, the temperature gradient with increasing distance from the cutting edge could be observed. Due to the large distance of the sensors to the cutting edge, steady state temperatures were not reached in the short amount of time, as the generated heat of the tool-chip contact propagates through the insert. In Fig. 9a, the temperature rises faster with increasing cutting speed. In Fig. 9b, measurements for a variation in feed rate are depicted. It results in a much faster temperature rise for a feed rate of 0.2 mm/rev compared to a feed rate of 0.1 mm/rev. For the measurement of TM1 with 0.1 mm/rev feed rate, the cutting length was shorter compared to the other measurements, resulting in a reduced cutting time.



(a) Variation of the cutting speed



(b) Variation of the feed rate

Fig. 9 Temperature measurement with thin-film sensors

6 Conclusions

Two concepts of piezoresistive thin-film sensors for in-process measurement of cutting forces were developed, sensors were fabricated, and their functionality was tested in machining experiments. Compared with traditional dynamometric plates, the sensor presented is much more flexible, since it is integrated in the cutting tool system.

Results of a DLC-based piezoresistive sensor compared well with the reference signal concerning response time and latency. But it showed the need to further improve the temperature compensation and calibration process as calculated forces drifted to false values shortly after the start of the process. A redesign of the temperature compensation is proposed in the outlook. Combined with a future calibration of the sensor in the machine it might lead to better results.

A manganin-based thin-film sensor was able to successfully measure steady state forces with a systematic error of 10–20% in comparison with a dynamometric platform. The sensor showed a fast response time at the beginning of the process as well as good repeatability. While heat also impacted this sensor type, a temperature compensation model was implemented and led to temperature independent results. Further enhancements, targeting the correction of systematic deviations in force values and the integration of temperature compensation within the thin-film system, are discussed in the outlook section.

Furthermore, a process to fabricate thermoresistive thin-film sensors on the rake face of cutting inserts with chip breaker geometry was successfully developed and implemented. The direct structuring of an electrophoretic resist using a laser opens up many possibilities to structure complex three-dimensional surfaces. This allows quick adjustments of the sensor design without the need to manufacture expensive exposure masks while still being able to generate structures of down to 10 μm . Experimental tests in turning operations showed the ability of the thin-film sensors to detect the temperature gradient in relation to the distance from the cutting edge. These results will be especially helpful for the further development, transfer and up-scaling of thin-film sensors on industrial cutting inserts.

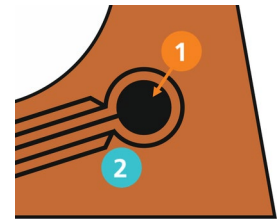
7 Outlook

In this section, optimizations of the presented thin-film sensors are presented.

The major challenge with the presented DLC thin-film sensor technology for cutting force measurement arises due to different temperatures at the force and TC structures during the process, leading to large deviations. To address this, the sensor design could be adapted by placing the force and TC structures in close proximity to each other. Since the TC structure must not be loaded, a profiled washer would still act as a heat sink and lead to differing temperatures. Alternatively, a temperature sensor with minimal force dependency could be placed in the vicinity of the force sensor instead of a TC structure but would also be loaded. Such a sensor could be a PTC sensor placed between the lower and upper insulation and wear-protection layer of the piezoresistive thin-film system. Figure 10 shows the suggested design of a force sensing structure and a surrounding temperature sensor. The temperature measured by this sensor could be used to compensate the temperature influence on the force sensor by using its thermoresistive characteristic.

The presented method for temperature compensation of the manganin sensor proved to be successful but could be implemented more efficiently and reliably by combining

Fig. 10 Force sensor (1) with surrounding temperature sensor (2)



both thin-film systems. Similar to the DLC thin-film system of Fig. 1a, the manganin sensor would be placed on the level of the conducting paths (2). This way, a DLC sensor for temperature compensation and a manganin meander structure could be placed above each other. Both sensors would be subjected to the same temperature. To prevent a short circuit between the manganin sensor and the underlying electrode of the DLC sensor, the intermediate insulating layer would have to be increased in thickness.

The findings presented highlight the need for future force sensor calibration to be performed directly on the turning machine. It is recommended to utilize temperature-compensated steady-state values instead of focusing solely on the force rise, aiming to prevent potential systematic deviations in force measurements.

Regarding the thermoresistive thin-film sensors, the objective is to position them in closer proximity to the cutting edge and potentially within the tool-chip contact zone. The durability of the sensors will also be part of further investigations. Additionally, the performance of these thin-film sensors will be assessed under wet cutting conditions. Thanks to the presence of a top insulating and wear-protective layer coating for all sensors, the cutting fluid is expected to not impact the measurements. Comparable thin-film systems have already been employed for temperature measurements in lubricated contacts, providing a basis for this expectation [16].

Author Contributions Conceptualization: M.P., G.G., V.S. and G.B.; Methodology: M.P., G.G. and C.P.; Investigation: M.P., G.G. and C.P.; Formal analysis: M.P.; Writing-original draft preparation: M.P., G.G. and C.P.; Writing-review and editing: A.S., V.S. and G.B.; Funding acquisition: V.S. and G.B.; Supervision: A.S., V.S. and G.B. All authors read and approved the final manuscript.

Funding Open Access funding enabled and organized by Projekt DEAL. The scientific work has been supported by the German Research Foundation, Deutsche Forschungsgemeinschaft (DFG) within the research priority program SPP2086 "Surface Conditioning in machining" (SCHU 1010/63-2 and BR 2178/47-2). The authors thank the DFG for the funding and intensive technical support. Open Access funding was enabled and organized by Projekt DEAL.

Declarations

Conflict of interest The Authors declare that they have no conflict of interest.

Open Access This article is licensed under a Creative Commons Attribution 4.0 International License, which permits use, sharing, adaptation, distribution and reproduction in any medium or format, as long as you give appropriate credit to the original author(s) and the source, provide a link to the Creative Commons licence, and indicate if changes were made. The images or other third party material in this article are included in the article's Creative Commons licence, unless indicated otherwise in a credit line to the material. If material is not included in the article's Creative Commons licence and your intended use is not permitted by statutory regulation or exceeds the permitted use, you will need to obtain permission directly from the copyright holder. To view a copy of this licence, visit <http://creativecommons.org/licenses/by/4.0/>.

References

- Klocke F, Kuljanic E, Veselovac D, Sortino M, Wirtz G, Totis G (2008) Development of an intelligent cutter for face milling. *Strain* 14:15
- Drossel W-G, Gebhardt S, Bucht A, Kranz B, Schneider J, Ettrichrätz M (2018) Performance of a new piezoceramic thick film sensor for measurement and control of cutting forces during milling. *CIRP Ann* 67(1):45–48. <https://doi.org/10.1016/j.cirp.2018.04.115>
- Panesso M, Ettrichrätz M, Gebhardt S, Georgi O, Rüger C, Gnauck M, Drossel W-G (2022) Design and characterization of piezoceramic thick film sensor for measuring cutting forces in turning processes. *Global conference on sustainable manufacturing*. Springer International Publishing, Cham, pp 30–39. https://doi.org/10.1007/978-3-031-28839-5_4
- Cheng Y, Wu W, Liu L, He Z, Song D (2022) Structural design and optimization of a turning tool embedded with thin-film strain sensors for in-process cutting force measurement. *AIP Adv*. <https://doi.org/10.1063/5.0079837>
- Biehl S, Paetsch N, Meyer-Kornblum E, Brauer G (2016) Wear resistant thin film sensor system for industrial applications. *Int J Instrum Meas* 1:6–11
- Biehl S, Rumposch C, Paetsch N, Bräuer G, Weise D, Scholz P, Landgrebe D (2016) Multifunctional thin film sensor system as monitoring system in production. *Microsyst Technol* 22:1757–1765. <https://doi.org/10.1007/s00542-016-2831-5>
- Kukhar' V (1972) Alloys for precision resistors. *Met Sci Heat Treat* 14(5):413–418. <https://doi.org/10.1007/BF00649823>
- Rostocki AJ, Urbański MK, Wiśniewski R, Wilczyńska T (2005) On the improvement of the metrological properties of manganin sensors. *Metrologia* 42(6):250–252. <https://doi.org/10.1088/0026-1394/42/6/S24>
- Safa M, Anderson J, Leather J (1982) Transducers for pressure, temperature and oil film thickness measurement in bearings. *Sens Actuators* 3:119–128. [https://doi.org/10.1016/0250-6874\(82\)80013-9](https://doi.org/10.1016/0250-6874(82)80013-9)
- Kagerer E (1991) Messung von elasto-hydrodynamischen parametern im hochbelasteten scheiben-und zahnkontakt. PhD thesis, Technische Universität München
- González G, Plogmeyer M, Schoop J, Bräuer G, Schulze V (2023) In-situ characterization of tool temperatures using in-tool integrated thermoresistive thin-film sensors. *Prod Eng Res Devel* 17(2):319–328. <https://doi.org/10.1007/s11740-023-01186-7>
- Werschmoeller D, Li X, Ehmann K (2012) Measurement of transient tool-internal temperature fields during hard turning by insert-embedded thin film sensors. *J Manuf Sci Eng* 134(6):061004. <https://doi.org/10.1115/1.4007621>
- Hayashi M, Yoshioka H, Shinno H (2008) An adaptive control of ultraprecision machining with an in-process micro-sensor. *J Adv Mech Des Syst Manuf* 2(3):322–331. <https://doi.org/10.1299/jamdsm.2.322>
- Ottermann R, Steppeler T, Dencker F, Wurz MC (2022) Degeneration effects of thin-film sensors after critical load conditions of machine components. *Machines* 10(10):870. <https://doi.org/10.3390/machines10100870>
- Steinhart JS, Hart SR (1968) Calibration curves for thermistors. *Deep Sea Res Oceanogr Abstr* 15:497–503. [https://doi.org/10.1016/0011-7471\(68\)90057-0](https://doi.org/10.1016/0011-7471(68)90057-0)
- Emmrich S, Plogmeyer M, Bartel D, Herrmann C (2021) Development of a thin-film sensor for in situ measurement of the temperature rise in rolling contacts with fluid film and mixed lubrication. *Sensors* 21(20):6787. <https://doi.org/10.3390/s21206787>